Bioorganic & Medicinal Chemistry 19 (2011) 623–630

Contents lists available at ScienceDirect

Bioorganic & Medicinal Chemistry

journal homepage: www.elsevier.com/locate/bmc

Cytotoxicity of δ-tocotrienols from *Kielmeyera coriacea* against cancer cell lines

Mariana Laundry de Mesquita [a], Renata Mendonça Araújo [b], Daniel Pereira Bezerra [c], Raimundo Braz Filho [d], José Elias de Paula [e], Edilberto Rocha Silveira [b], Cláudia Pessoa [c], Manoel Odorico de Moraes [c], Letícia Veras Costa Lotufo [c], Laila Salmen Espindola [a,*]

[a] *Laboratório de Farmacognosia, Universidade de Brasília, Brasília, Brazil*
[b] *Departamento de Química Orgânica e Inorgânica, Universidade Federal do Ceará, Fortaleza, Brazil*
[c] *Departamento de Fisiologia e Farmacologia, Universidade Federal do Ceará, Fortaleza, Brazil*
[d] *FAPERJ/UENF/UFRRJ, Rio de Janeiro, Brazil*
[e] *Laboratório de Anatomia Vegetal, Universidade de Brasília, Brasília, Brazil*

ARTICLE INFO

Article history:
Received 16 July 2010
Revised 14 October 2010
Accepted 18 October 2010
Available online 25 October 2010

Keywords:
Kielmeyera coriacea
HL-60
DNA synthesis
δ-Tocotrienols
Apoptosis
Necrosis

ABSTRACT

In the search for new anti-cancer compounds, Brazilian Cerrado plant species have been investigated. The hexane root bark extract of *Kielmeyera coriacea* lead to a mixture of δ-tocotrienol (**1**) and its dimer (**2**). The structures of both compounds **1** and **2** were established based on detailed 1D and 2D NMR and EI-MS analyses. The cytotoxicity of the mixture was tested against four human tumor cell lines in the following cultures: MDA-MB-435 (melanoma), HCT-8 (colon), HL-60 (leukemia), and SF-295 (glioblastoma), and displayed IC_{50} values ranging from 8.08 to 23.58 μg/mL. Additional assays were performed in order to investigate the mechanism of action of the mixture (**1** + **2**) against the human leukemia cell line HL-60. The results suggested that the mixture suppressed leukemia growth and reduced cell survival, triggering both apoptosis and necrosis, depending on the concentration.

1. Introduction

Cancer affects about two hundred different types of cells. The most prominent characteristics of the disease are lack of control in cell proliferation, cell differentiation, and cell mortality, invading either organs or tissues.[1] There are many difficulties in the treatment of cancer, but the most concerning are drug resistance, toxicity and low specificity.

The potential to find out promising molecules in the Cerrado biome to several applications have already been demonstrated in diverse biological models.[2–5] Four hundred and twelve crude extracts from Brazilian Cerrado native plants were previously assayed against cancer cell lines.[3] The hexane extract from *Kielmeyera coriacea* Mart. & Zucc. (Calophyllaceae) root bark, known in Brazil as 'pau-santo', showed significant activity.[3] This extract showed IC_{50} values of 10.6 μg/mL for MDA-MB-435 (melanoma), 5.2 μg/mL for HCT-8 (colon), 15.4 μg/mL for HL-60 (leukemia), and 6.4 μg/mL for SF-295 (glioblastoma) cells, and was, therefore, selected for this study.

2. Results and discussion

Bioassay-guided fractionation of the hexane root bark extract of *K. coriacea* resulted in a mixture of two compounds, whose physical and spectral data revealed the presence of a monomer of δ-tocotrienol (**1**) and a novel δ-tocotrienol peroxy-dimer (**2**).

2.1. Characterization of δ-tocotrienol (1) and δ-tocotrienol peroxy-dimer (2)

Compound **1** was obtained as a brown viscous liquid. Spectral data, mainly 1D and 2D NMR ^1H (1D ^1H and 2D ^1H-^1H-COSY), ^{13}C (CPD = Composite Pulse in broadband Decoupling and DEPT), HSQC (Heteronuclear Single Quantum Coherence allowed the assignment of all hydrogenated carbon atoms), HMBC (Heteronuclear Multiple Bond Correlation involving two, $^2J_{CH}$, and three, $^3J_{CH}$, bonds, Table 1), NOESY (Nuclear Overhauser Effect Spectroscopy) and mass (EI-MS, 70 eV) spectra, compared with the literature values[6] were used to characterize **1** as δ-tocotrienol, including the same relative stereochemistry. The results of the extensive applications of 1D and 2D NMR were also used to establish unequivocally the complete ^1H and ^{13}C resonance assignments, as summarized in Table 1.

The mass spectrum exhibited a base peak at *m/z* 396 (EI-MS, 70 eV) corresponding to δ-tocotrienol (**1**) (Fig. 1). The presence of the peak at *m/z* 791, compatible with a molecular formula of

* Corresponding author. Address: Campus Universitário Darcy Ribeiro, Asa Norte, Postal Code 70910-900 Brasília, DF, Brazil. Tel.: +55 61 3307 3046; fax: +55 61 3107 1943.
E-mail address: darvenne@unb.br (L.S. Espindola).

0968-0896/$ - see front matter © 2010 Elsevier Ltd. All rights reserved.
doi:10.1016/j.bmc.2010.10.044

Table 1
NMR data for δ-tocotrienol (**1**) and δ-tocotrienol peroxy-dimer (**2**) (in $CDCl_3$ and pyridine-d_5 as solvents). Residual $CHCl_3$/$CDCl_3$ or pyridine-d_5 used as reference. Chemical shifts (δ, ppm) and coupling constants (J, Hz, in parenthesis)[a]

Atom number	**2**		**1**			
			HSQC		HMBC	
	δ_C	δ_H	δ_C	δ_H	$^2J_{CH}$	$^3J_{CH}$
2/2″	75.74	—	75.52	—	2H-3; 2H-1′; 3H-2a	2H-4; 2H-2′
2a/2″a	24.55	1.30, 3H, s	24.21	1.25, 3H, s		2H-3; 2H-1′
3/3″	32.19	1.75, 2H, m	31.58	1.79, 2H, m	2H-4	3H-2a
4/4″	23.20	2.73, 2H, m	22.68	2.70, 2H, m	2H-3	H-5
5/5″	114.20	6.87, 1H, d, 2.6	112.84	6.37, 1H, d, 2.6		2H-4; H-7
6/6″	151.74	—	148.00	—	H-5; H-7	
7/7″	117.30	7.01, 1H, d, 2.6	115.90	6.49, 1H, d, 2.6		H-5; 3H-8a
8/8″	127.38	—	127.91	—	3H-8a	
8a/8″a	16.48	2.32, 3H, s	16.19	2.14, 3H, s		H-7
9/9″	145.71	—	146.16	—		H-5; H-7; 2H-4; 3H-8a
10/10″	122.02	—	121.42	—	2H-4	2H-3
1′/1‴	40.40	1.67, 1H, m and 1.61, 1H, m	39.90	1.65, 2H, m and 1.55, 2H, m	2H-2′	2H-3; 3H-2a
2′/2‴	22.99	2.12-2.16, 2H, m	22.37	2.09, 2H, m	2H-1′; H-3′	
3′/3‴	125.31	5.16, 1H, t, 6.7	124.51	5.16, 1H, t, 6.7	2H-2′	3H-4′a; 2H-5′
4′/4‴	[b]	—	135.15	—	2H-5′; 3H-4′a	2H-2′; 2H-6′
4′a/4‴a	16.82	1.69, 3H, m	16.24	1.61, 3H, s		H-12; 2H-5′
5′/5‴	40.39	1.98–2.01, 2H, m	39.90	1.99, 2H, m		H-3′; H-7′; 3H-4′a
6′/6‴	27.46	2.07–2.10, 2H, m	26.96	2.05, 2H, m	2H-5′	
7′/7‴	125.11	5.13, 1H, t, 6.0	124.50	5.12, 1H, m	2H-6′	2H-5′; 2H-9′
8′/8‴	[b]	—	135.31	—	3H-8′a; 2H-9′	2H-6′; 2H-10′
8′a/8‴a	16.33	1.69, 3H, s	16.06	1.62, 3H, s		H-7′; 2H-9′
9′/9‴	40.40	1.98–2.01, 2H, m	39.90	1.99, 2H, m		H-7′; H-11′
10′/10‴	27.30	2.12–2.16, 2H, m	26.80	2.05, 2H, m	2H-9′; H-11′	
11′/11‴	125.40	5.12, 1H, t, 6.0	124.62	5.12, 1H, m	2H-10′	2H-9′; 3H-12′a; 3H-12′b
12′/12‴	131.56	—	131.44	—	3H-12′a; 3H-12′b	2H-10′
12′a/12‴a	18.10	1.61, 3H, s	17.87	1.62, 3H, s		H-11′; 3H-12′b
12′b/12‴b	26.14	1.70, 3H, s	25.89	1.70, 3H, s		H-11′; 3H-12′a

[a] Number of hydrogen bound to carbon atoms deduced by comparative analysis of {^{1}H}- and DEPT-^{13}C NMR spectra. Chemical shifts and coupling constants (J) were obtained from 1D ^{1}H NMR spectrum. ^{1}H–^{1}H-COSY experiment was also used to make the assignments. Superimposed ^{1}H signals are described without multiplicity and chemical shifts were deduced by ^{1}H–^{1}H-COSY, HSQC, and HMBC spectra.
[b] Superimposed with pyridine signal.

$C_{54}H_{78}O_4$, was attributed to the molecular ion δ-tocotrienol peroxy-dimer (**2**) (Fig. 1).

Compound **2** was obtained as a brown viscous liquid after separation through HPLC chromatography (265 nm) from the mixture of both δ-tocotrienol (**1**) and δ-tocotrienol peroxy-dimer (**2**).

Comparative analysis of the NMR spectra of **1** and **2** (Table 1) revealed as significant differences the changes observed in the ^{1}H and ^{13}C of the signals of the CH-7 [δ_C 115.90 (**1**)/117.30 (**2**), $\Delta\delta_C$ = 1.40 ppm], C-6 [δ_C 148.00 (**1**)/151.78 (**2**), $\Delta\delta_C$ = 3.78 ppm] and CH-5 [δ_C 112.84 (**1**)/114.20 (**2**), $\Delta\delta_C$ = 1.36 ppm] and the hydrogen atoms H-7 [δ_H 6.49 (**1**)/7.01 (**2**), $\Delta\delta_H$ = 0.52 ppm], H-5 [δ_H 6.37 (**1**)/6.87 (**2**), $\Delta\delta_H$ = 0.50 ppm], in the agreement with the deshielding caused by the decreasing electronic donating ability of the C-6 hydroxyl after the formation of the peroxy bridge in **2**. This deduction in combination with the additional NMR data spectral (Table 1) and mass spectrum of **2** (*m/z* 791 $[M]^+$, Scheme 1) were used to establish the structure of this new compound isolated from *K. coriacea* as the δ-tocotrienol peroxy-dimer (**2**, Fig. 1). These spectral data were also used to eliminate structural dimer alternatives **I**, **II**, and **III** (Fig. 1). Thus, the tocotrienols isolated from *K. coriacea* were characterized as δ-tocotrienol monomer, 2,8-dimethyl-2-[(3*E*,7*E*)-4,8,12-trimethyltrideca-3,7,11-trienyl] chroman-6-ol (**1**), and δ-tocotrienol peroxy-dimer, bis-(6,6′-*O*-*O*)-2,8-dimethyl-2-[3(*E*),7(*E*),4,8,12-trimethyl-trideca-3,7,11-trienyl]-chromane (**2**), shown in Figure 1.

2.2. Evaluation of δ-tocotrienols cytotoxicity

The cytotoxicity of the test mixture (**1** + **2**) was investigated against four tumor cell lines: HL-60 (leukemia), HCT-8 (colon), MDA-MB-435 (melanoma), and SF-295 (glioblastoma) cell lines. To access the selectivity of the tested compounds, cytotoxicity was further evaluated against two normal cell lines: NIH-3T3 and peripheral blood mononuclear cells (PBMC).

These four tumor cell lines were incubated with increasing concentrations of the mixture (**1** + **2**) for 72 h at 37 °C and analyzed using the tetrazolium salt colorimetric MTT assay. Significant dose-dependent suppression of cell growth was observed. Table 2 displays the IC_{50} values, which ranged from 8.08 to 23.58 μg/mL. In HCT-8 and MDA-MB-435 cells, the crude extract was more active. These results agree with previous reports that δ-tocotrienols exert stronger anti-proliferative effects against human hepatoma Hep3B cells,[7] HepG2 cells,[8] and murine hepatoma MH134 cells both in vitro and in vivo.[9] In order to study the mechanisms involved in the cytotoxicity of δ-tocotrienols, the mixture (**1** and **2**) at concentrations of 5 and 10 μg/mL was tested in HL-60 cells.

Cell viability was reduced at both concentrations as demonstrated by the trypan blue exclusion test (Fig. 2A). However, only the highest concentration of the mixture (**1** + **2**) caused a significant increase in the number of non-viable cells. Additionally, DNA synthesis was affected after treatment with the mixture (**1** + **2**), resulting in a lower amount of cell division that corroborated with the trypan blue exclusion test and MTT assay. The mixture (**1** + **2**) inhibited BrdU incorporation by 23.4% and 95.9% at the concentrations of 5 and 10 μg/mL, respectively (Fig. 2B). The doxorubicin positive control reduced DNA synthesis by 47.9%.

Cell cycle progression was determined using flow cytometry. These results suggest that the mixture may preferentially stimulate cells in the G_2/M phase to undergo apoptosis more readily. At the 5 μg/mL concentration, the number of cells in G_0/G_1 phase and S phase remained constant. However, there were only 8.78% in the G_2/M phase, as opposed to 15.49% in the negative control.

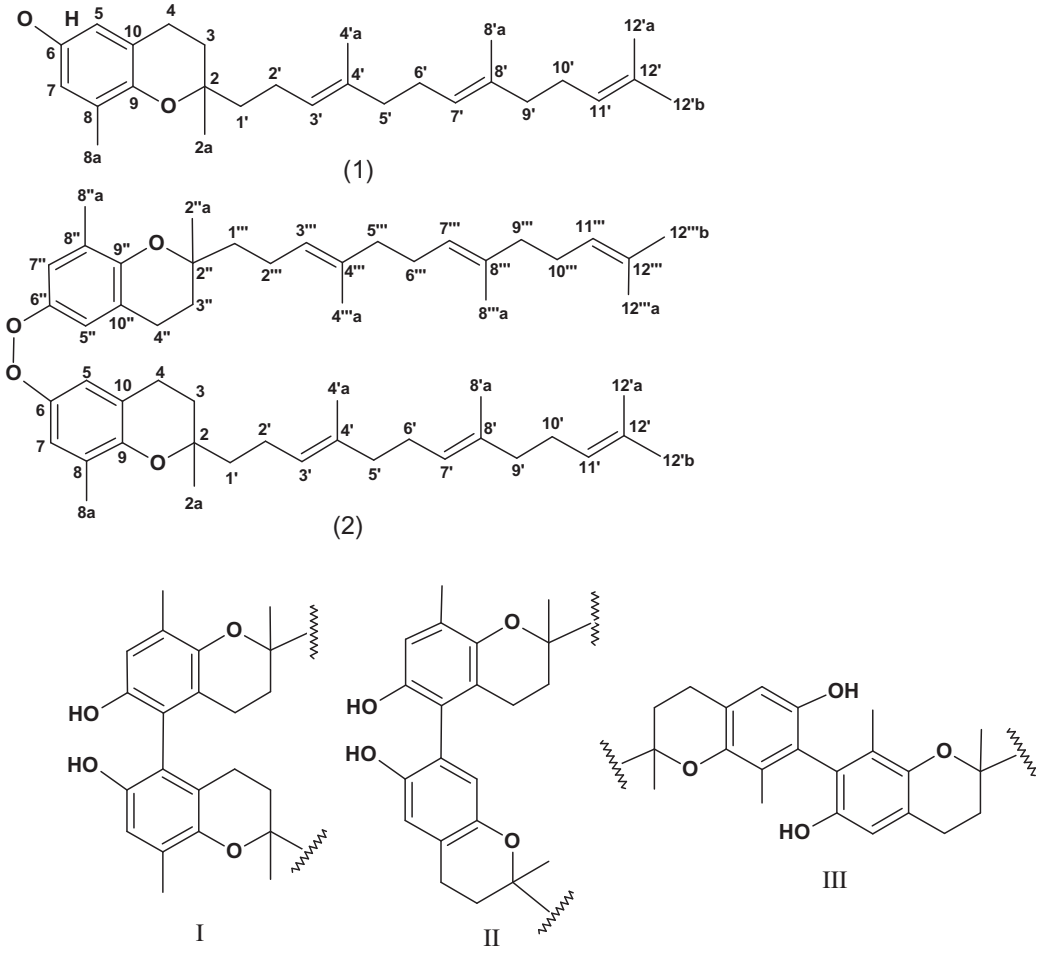

Figure 1. Molecular structure of δ-tocotrienol monomer (**1**) and δ-tocotrienol peroxy-dimer (**2**) and discarded structural possibilities showing C–C bridges (I, II, and III).

At the 10 μg/mL concentration, the percentage of cells was significantly lower in all phases (Table 3). In addition, both concentrations caused significant internucleosomal DNA fragmentation (Fig. 3A). The doxorubicin positive control also demonstrated significant internucleosomal DNA fragmentation.

Understanding the regulatory mechanism through the control of cell cycle progression and growth could play a critical role in the development of new agents to prevent and treat cancer. It has been demonstrated that δ-tocotrienol treatment led to the down-regulation of cyclin B1 and CDK1, in MDA-MB-231 breast cancer cells, that are required for the progression of the cell cycle through the G2/M checkpoint. Negative regulation of these cell cycle promotes an increase in G1 and G2/M arrest following the addition of δ-tocotrienol.[10] This work suggests that the mixture of δ-tocotrienol (**1**) and its peroxy-dimer (**2**) may preferentially stimulate cells in the G_2/M phase to undergo apoptosis in human leukemia cell line HL-60.

Additional experiments were performed to investigate whether the inhibitory growth activity of the mixture (**1** + **2**) was related to the induction of apoptosis or necrosis. The reduction of the number of cells was also observed by flow cytometry analyses in both concentrations (Fig. 3B). On the other hand, the mixture (**1** + **2**) only induced disruption of membrane integrity at 10 μg/mL (Fig. 3C). Furthermore, the mixture caused cell shrinkage at both concentrations (data not shown). This was supported by a decrease in forward light scatter (FSC) and nuclear condensation as observed by a transient increase in side scatter (SSC). Both of the aforementioned morphological modifications are compatible with cell apoptosis. The mixture also induced mitochondrial depolarization in HL-60 cells, which was observed by the incorporation of rhodamine 123 (Fig. 3D). Doxorubicin also induced apoptotic effects.

Morphological examination of treated and untreated HL-60 cells revealed severe drug-mediated changes, as observed by light microscopy (qualitative analyses, Fig. 4) and fluorescent microscopy (quantitative analyses, Fig. 5). In light microscopy analyses, HL-60 cells incubated with the mixture (**1** + **2**) at 5 μg/mL showed morphologies consistent with apoptosis, including chromatin condensation and fragmentation of the nuclei. However, these cells at a concentration of 10 μg/mL were induced to a reduction in the volume, destabilization of the plasma membrane and pyknotic nuclei, all of which are morphological features consistent with necrosis. In fluorescent microscopy analyses, the percentage of viable, apoptotic and necrotic cells were calculated. After treatment of HL-60 cells with the mixture for 24 h at 37 °C, an increasing number of apoptotic and necrotic cells were observed (p <0.05). In addition, the doxorubicin-treated cells also showed apoptotic characteristics.

Apoptosis induction is arguably the most potent defense against cancer progression. Researchers have demonstrated that tocotrienols induce apoptosis in cancer cell lines.[11,12] However, the exact mechanisms triggered by tocotrienols have not been fully elucidated to date. Tocotrienols induce caspase-9 expression in human colon carcinoma cells via the activation of p53 and an increase in the Bax/Bcl-2 ratio.[13] δ-Tocotrienol-induced apoptosis also seemed to be involved in the activation of transforming growth factor signaling pathways growth factor-β, Fas and JNK in human breast cancer cells.[14] Sakai et al.[7] reported that caspase-3, caspase-8 and

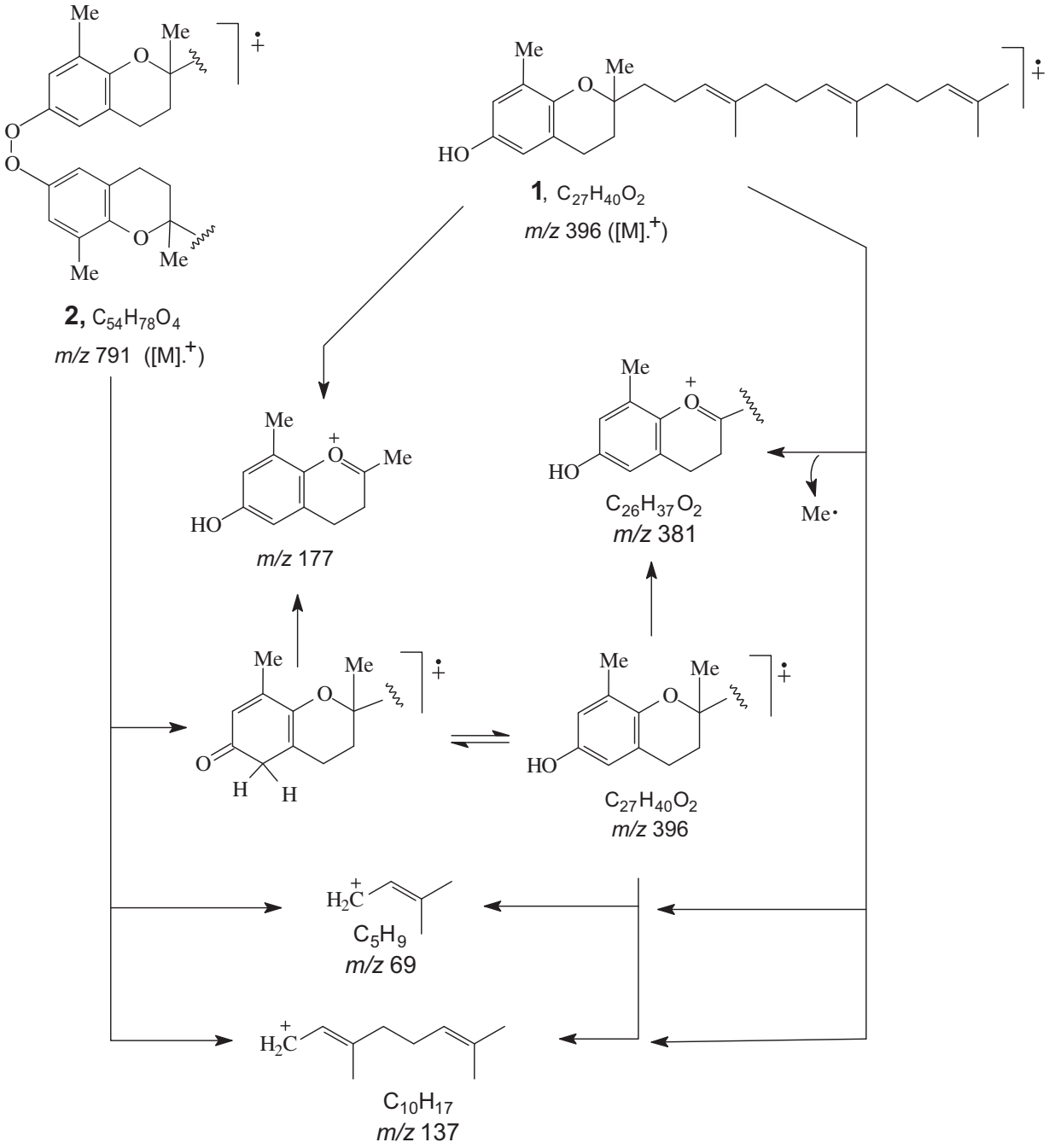

Scheme 1. Proposed mechanisms for the fragmentation of both **1** and **2** in the mass spectrometer (70 eV). Only peaks classified as principals are shown.

Table 2
Cytotoxic activity of the mixture (**1** + **2**) on human cancer cell lines

Cell line	Histotype	Mixture (**1** + **2**) (μg/mL)	Doxorubicin (μg/mL)
HL-60	Leukemia	8.08 6.53–9.99	0.02 0.01–0.03
HCT-8	Colon	13.02 11.55–16.27	0.01 0.01–0.02
SF-295	Glioblastoma	23.58 20.11–26.05	0.24 0.17–0.36
MDA-MB-435	Melanoma	16.39 14.56–19.12	0.48 0.34–0.66

Doxorubicin was used as a positive control. Data are presented as IC_{50} values and 95% confidence interval (CI 95%) from three independent experiments, performed in duplicate.

Table 3
Effect of the mixture (**1** + **2**) on different stages within the HL-60 cell cycle determined by flow cytometry using propidium iodide, triton X-100, and citrate after 24 h at 37 °C

Sample	Concentration (μg/mL)	Phase of the cell cycle (%)		
		G_0/G_1	S	G_2/M
Control	—	56.84 ± 1.25	18.12 ± 0.43	15.49 ± 1.04
Doxorubicin	0.3	13.86 ± 2.26[a]	1.17 ± 0.18[a]	0.481 ± 0.07[a]
1 + **2**[b]	5	51.56 ± 1.99	17.00 ± 1.06	8.78 ± 0.62[a]
	10	22.47 ± 2.73[a]	2.00 ± 0.51[a]	0.72 ± 0.15[a]

Negative control (control) was treated with the vehicle used for diluting the tested substance. Doxorubicin was used as a positive control. Data are presented as mean values ± SEM from three independent experiments performed in triplicate. Five thousand events were analyzed in each experiment.

[a] p <0.05 compared to control by ANOVA followed by Student Newman Keuls test.

[b] **1** + **2** δ-Tocotrienol monomer (**1**) and δ-tocotrienol peroxy-dimer (**2**) mixture.

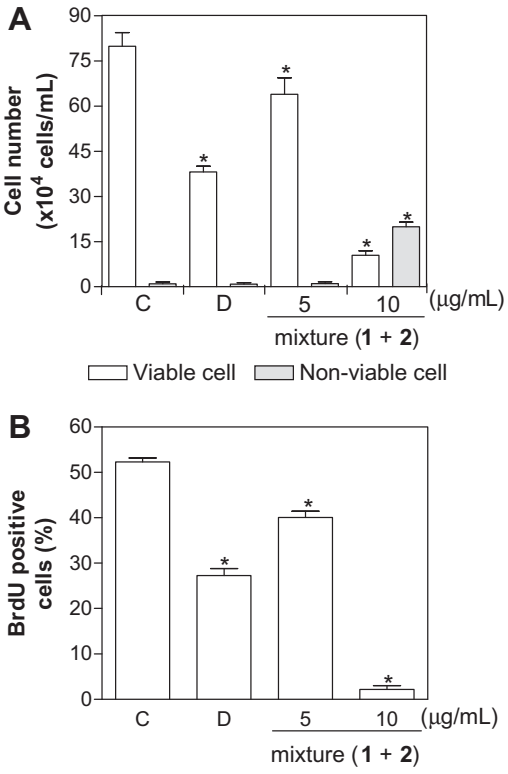

Figure 2. Effect of the mixture **(1 + 2)** on HL-60 cell proliferation after 24 h incubation. (A) Cell proliferation determined by trypan blue staining. (B) Cell proliferation determined by 5-bromo-2′-deoxyuridine (BrdU) incorporation. Negative control (C) was treated with the vehicle used for diluting the tested substance. 0.3 mg/mL doxorubicin was used as a positive control (D). Data are presented as mean values ± SEM from three independent experiments performed in triplicate. $^{*}p$ <0.05 compared to control by ANOVA followed by Student Newman Keuls test.

caspase-9 were involved in γ-tocotrienol-induced apoptosis of Hep3B cells, and that Bax and Bid participated in the regulation of apoptosis induction. Ahn et al.[15] showed that γ-T3 inhibited the NF-κB activation pathway through inhibition of RIP and TAK1, leading to suppression of antiapoptotic gene products and potentiation of apoptosis. Therefore, the mixture of δ-tocotrienol (**1**) and its peroxy-dimer (**2**) induce apoptosis via mitochondrial pathways, and necrosis, depending on the concentration used against the human leukemia cell line HL-60. Evaluation of the mixture in NIH-3T3 mammalian fibroblast cells and in lymphocytes showed IC_{50} values of 15.43 and 12.11 μg/mL, respectively, which indicated there was no selectivity to cancer cells. However, natural products could be used in the design of a more potent and selective agent.

3. Conclusion

A mixture of δ-tocotrienol (**1**) and its peroxy-dimer (**2**) from the *K. coriacea* hexane root bark extract was found to be active against MDA-MB-435 (melanoma), HCT-8 (colon), HL-60 (leukemia), and SF-295 (glioblastoma) cells. The mixture (**1** + **2**) suppressed leukemia growth and reduced cell survival, triggering both apoptosis and necrosis, at concentrations of 5 and 10 μg/mL, respectively.

4. Experimental

4.1. General experimental procedures

The mass spectra were obtained using a Hewlett–Packard 5971 mass spectrometer by electron impact ionization (70 eV). ^{1}H and ^{13}C nuclear magnetic resonance (NMR) were recorded on a Bruker Avance DRX-500 (500 MHz for ^{1}H and 125 MHz for ^{13}C). Chemical shifts are given in ppm relative to residual $CHCl_3/CDCl_3$ (δ_H 7.24/δ_C 77.23, central signal of the triplet related to carbon) or pyridine-d_5 [δ_H 8.74 (H-2/H-6)/δ_C 150.6 (C-2/C-6), δ_H 7.58 (H-4)/δ_C 135.9 (C-4) and δ_H 7.22 (H-3/H-5)/δ_C 123.9 (C-3/C-5)]. Silica Gel 60 (2–25 mesh, Merck) was used for analytical TLC. Silica Gel 60 (40–63 mesh, Merck) was used for column flash chromatography. All compounds were visualized on TLC by spraying with vanillin/perchloric acid/EtOH, followed by heating. This mixture was further purified through preparative HPLC (Waters-1525) connected to a detector PDAWaters-2996 (265 nm) with XTerra-SiO_2 column (4.6 × 250 mm, 5 μM).

4.2. Plant material

K. coriacea Mart. & Zucc. (Calophyllaceae) was collected from the Cerrado biome, in the outskirts of Brasília, Distrito Federal, Brazil, in 2005, and was identified by Dr. José Elias de Paula, from the Biology Institute of the University of Brasília. A voucher specimen was deposited in the Herbarium of said University, under the reference: J. Elias de Paula (UB) 3745.

4.3. Extraction and isolation

Dried and powdered root bark (340 g) of *K. coriacea* was submitted to successive extractions with hexane, through a maceration process, to yield a crude extract (28.85 g) following evaporation of the solvent under reduced pressure at 40 °C. An aliquot of this extract (4 g) was fractionated using silica gel by elution with a gradient of cyclohexane–EtOAc to afford 10 fractions (F1–F10) based on TLC behavior.

Fractions F3 and F4 showed higher cytotoxicity at 50 μg/mL. Results are stated for F3 and F4, respectively, against the following cell lines: SF-295 (95.87% and 78.83%), HCT-8 (96.94% and 80.39%), and MDA-MB-435 (98.87% and 96.02%).

Chromatography was performed on fraction 4 (F4, 900 mg) using silica gel with a gradient of hexane, CH_2Cl_2, and MeOH. Fourteen sub-fractions (F4–1 to F4–14) were collected. Successive purifications of sub-fraction F4–6 (220.6 mg) using silica gel with a gradient of hexane–$CHCl_3$ yielded a mixture of two compounds. 50.0 mg of the mixture was further purified through preparative HPLC using hexane/EtOAc (60:40) as eluent, to give the pure compounds **1** (41.35 mg; t_R = 8.3 min) and **2** (4.4 mg; t_R = 6.5 min).

The molecular formulas of the two aforementioned compounds were deduced to be $C_{27}H_{40}O_2$ corresponding to δ-tocotrienol (**1**), and $C_{54}H_{78}O_4$ corresponding to δ-tocotrienol peroxy-dimer (**2**).

4.3.1. δ-Tocotrienol, {1, 2,8-dimethyl-2-[3(*E*),7(*E*),4,8,12-trimethyltrideca-3,7,11-trienyl]-chroman-6-ol}

Brown viscous liquid; $[\alpha]_D^{20}$ −4 (*c* 0.05, $CHCl_3$); EI-MS *m*/*z*: 396 [M^+], 259, 217, 203, 192, 177, 163, 149, 137, 109, 95, 81, 69, 55, and 41. Table 1 presents ^{1}H and ^{13}C NMR spectral data.

4.3.2. δ-Tocotrienol peroxy-dimer {2, bis-(6,6′-*O*-*O*)-2,8-dimethyl-2-[3(*E*),7(*E*),4,8,12-trimethyl-trideca-3,7,11-trienyl]-chromane}

Brown viscous liquid; EI-MS *m*/*z*: 791 [M^+], 396, 259, 217, 203, 192, 177, 163, 149, 137, 109, 95, 81, 69, 55, and 41. Table 1 presents ^{1}H and ^{13}C NMR spectral data.

4.4. Cell lines and cell cultures

The cell lines used in this work—MDA-MB-435 (melanoma), HCT-8 (colon), HL-60 (leukemia), and SF-295 (glioblastoma)—were all obtained from the National Cancer Institute (Bethesda, MD, USA). These cells were maintained in RPMI 1640 medium supplemented

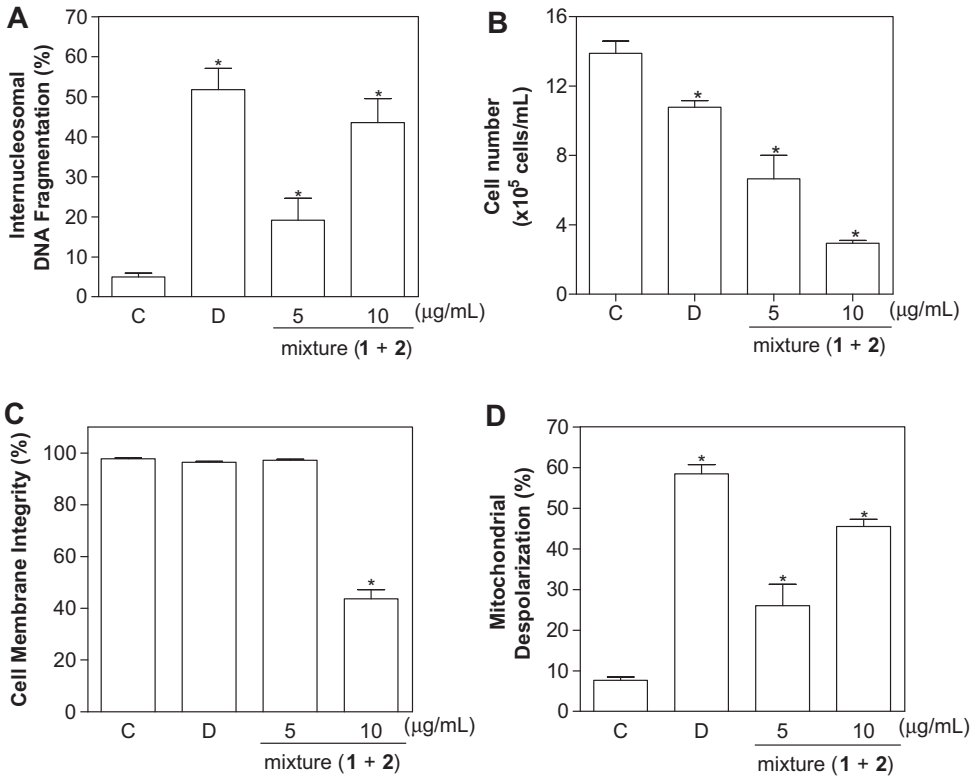

Figure 3. Effect of the mixture **(1 + 2)** on HL-60 cells after 24 h incubation determined by flow cytometry after 24 h at 37 °C. (A) Internucleosomal DNA fragmentation, (B) cell proliferation, (C) cell membrane integrity, and (D) mitochondrial transmembrane potential. Negative control (C) was treated with the vehicle used for diluting the tested substance. 0.3 mg/mL doxorubicin was used as a positive control (D). Data are presented as mean values ± SEM from three independent experiments performed in triplicate. $^{*}p$ <0.05 compared to control by ANOVA followed by Student Newman Keuls test.

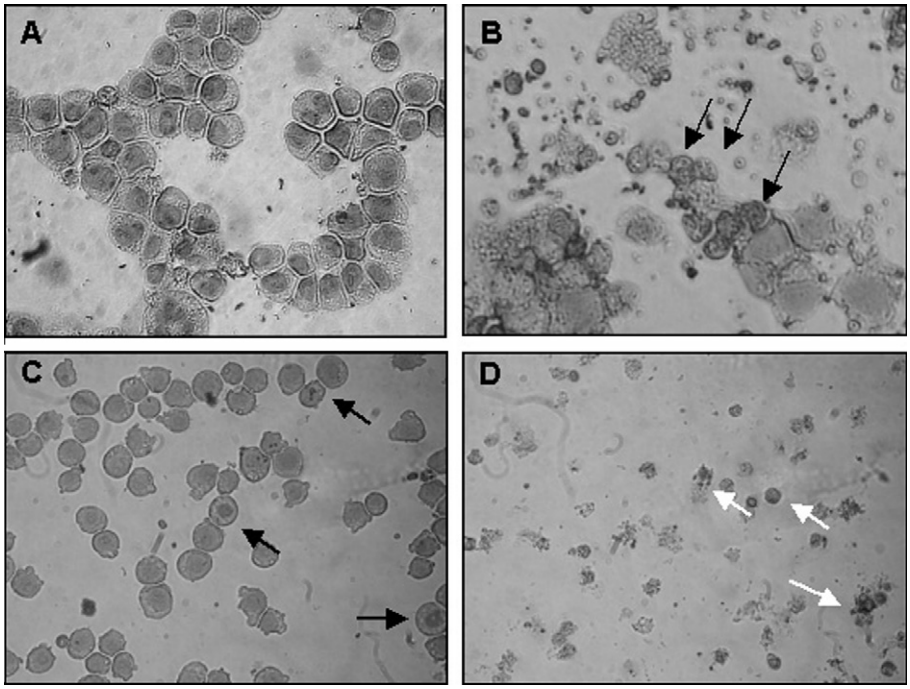

Figure 4. Light Microscopy (400×) of hematoxylin/eosin-stained HL-60 cells. Untreated cells—negative control (A), 0.3 μg/mL doxorubicin—positive control (B), mixture (**1 + 2**) at 5 μg/mL (C), and at 10 μg/mL (D). Black arrows show chromatin condensation or nuclear fragmentation, and white arrows show destabilization of the plasma membrane or pyknotic nuclei.

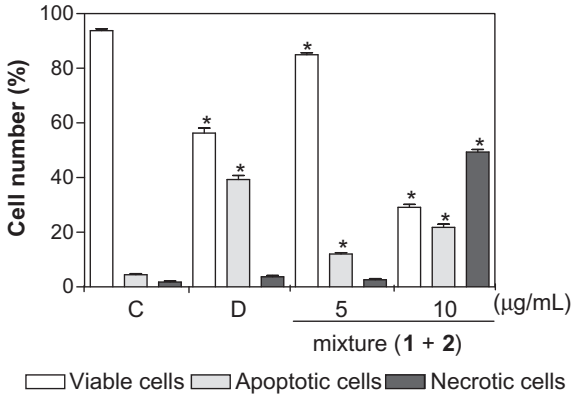

Figure 5. Fluorescence microscopy of HL-60 cells after 24 h at 37 °C using acridine orange and ethidium bromide. Negative control (C) was treated with the vehicle used for diluting the tested substance. 0.3 mg/mL doxorubicin was used as a positive control (D). Data are presented as mean values ± SEM from three independent experiments performed in triplicate. $^{*}p$ <0.05 compared to control by ANOVA, followed by Student Newman Keuls test.

with 10% fetal bovine serum, 2 mM glutamine, 100 U/mL penicillin, 100 μg/mL streptomycin at 37 °C with 5% CO_2.

4.5. Proliferation assay

4.5.1. Inhibition of tumor cell proliferation

Cytotoxicity of the test mixture (**1** + **2**) was investigated against HL-60, HCT-8, MDA-MB-435, and SF-295. For all experiments, these cells were transferred into 96-well plates (10^5 cells/well for adherent cells or 0.5×10^5 cells/well for suspended cells) in 100 μL of medium. After 24 h, serial dilutions (from 0.02 to 25.0 μg/mL) of the test mixture dissolved in DMSO were added to each well (using the HTS—high-throughput screening—Biomek 3000—Beckman Coulter, Inc. Fullerton, CA, USA) and incubated for 72 h. Doxorubicin (Sigma–Aldrich Co., St. Louis, MO, USA) was used as a positive control. Tumor cell growth was quantified by the ability of living cells to reduce the yellow dye 3-(4,5-dimethyl-2-thiazolyl)-2,5-diphenyl-2*H*-tetrazolium bromide (MTT) to a purple formazan product.[16] At the end of the incubation, plates were centrifuged and the medium was replaced with fresh medium (150 μL) containing MTT (0.5 mg/mL). Three hours later, the MTT formazan product was dissolved in 150 μL DMSO, and the absorbance measured using a multi-plate reader (DTX 880 Multimode Detector, Beckman Coulter, Inc., Fullerton, CA, USA). Cytotoxic activity was quantified as the percentage of control absorbance of reduced dye at 595 nm.

Cytotoxicity was evaluated over a concentration range of 300–9.4 μg/mL for NIH-3T3 cells. These cells were seeded in 96-well plates at a density of 8×10^3 cells in Dulbecco's Modified Eagle Medium (DMEM; Gibco®) containing 10% stain buffer (FBS) (v/v) overnight at 37 °C in 5% CO_2. The medium was changed and incubated with or without different concentrations of the mixture (**1** + **2**) at 37 °C in 5% CO_2. After 24 h, the cell viability was determined by MTT assay.[16] Briefly, 15 μL of MTT solution (5 mg/mL in PBS) were added to each well. After 3 h of incubation at 37 °C in 5% CO_2, the culture media was aspirated and 100 μL of DMSO were added. The absorbance was monitored using a spectrophotometer with a microplate reader at a wavelength of 595 nm.

Peripheral blood mononuclear cells (PBMC) were also tested. Heparinized blood from healthy, non-smoking donors who had not taken any drugs for at least 15 days prior to sampling was collected, and the PBMC were isolated via a standard method of density-gradient centrifugation over Ficoll-Hypaque. PBMC were washed and re-suspended at a concentration of 3×10^6 cells/mL in RPMI 1640 medium supplemented with 20% fetal bovine serum, 2 mM glutamine, 100 U/mL penicillin, and 100 μg/mL streptomycin at 37 °C with 5% CO_2. Phytohemagglutinin (4%) was added at the beginning of the experiment.

4.6. Study of the cytotoxic mechanism affecting the leukemia cell (HL-60)

The following experiments were performed in order to elucidate the mechanism(s) involved in the cytotoxic action of the mixture (**1** + **2**) using HL-60 cells (3×10^5 cells/mL), since it was the most sensitive cell line. Concentrations of 5 and 10 μg/mL were analyzed. 0.3 μg/mL doxorubicin was used as a positive control.

4.6.1. Trypan blue exclusion test

Cell viability was determined using the trypan blue exclusion test. Aliquots were removed from cultures after 24 h, and cells that excluded the trypan blue dye were counted in a Neubauer chamber.

4.6.2. Measurement of DNA synthesis

Ten microliters of 5-bromo-2′-deoxyuridine (BrdU, 10 mM) was added to each well and the plate was incubated for 3 h at 37 °C before completing the 24 h period of drug exposure. To assay the amount of BrdU incorporated into DNA, cells were harvested, transferred to cytospin slides, and allowed to dry for 2 h at room temperature. Cells that had incorporated BrdU were labeled by direct peroxidase immunocytochemistry utilizing chromogen diaminobenzidine. Slides were counterstained with hematoxylin, mounted, and cover slipped. Evaluation of BrdU positivity was performed using light microscopy (Olympus, Tokyo, Japan). Two hundred cells were counted per sample to determine the percentage of positive cells.

4.6.3. Cell cycle distribution and internucleosomal DNA fragmentation analyses

Based on the procedure of Nicoletti et al.,[17] HL-60 cells (3×10^5) were incubated at 37 °C for 24 h, without light, in a lysis solution containing 0.1% citrate, 0.1% Triton X-100, and 50 μg/mL propidium iodide. Cell fluorescence was then determined using flow cytometry in a Guava® EasyCyte™ Mini System cytometer (Guava Technologies, Inc., Industrial Blvd. Hayward, CA, USA) and the CytoSoft 4.1 software. Five thousand events were evaluated per experiment and cellular debris was omitted from the analysis. All DNA that was sub-diploid in size (sub-G_1) was considered the result of internucleosomal DNA fragmentation.

4.6.4. Cell membrane integrity

Cell membrane integrity was evaluated by the exclusion of 2 μg/mL propidium iodide. Cell fluorescence was determined using flow cytometry as in Section 4.6.3. Five thousand events were evaluated per experiment and cell debris was omitted from the analysis.

4.6.5. Measurement of mitochondrial transmembrane potential

Mitochondrial transmembrane potential was determined by the retention of rhodamine 123 dye by HL-60 cells. Cells were washed with phosphate-buffered saline (PBS), incubated with rhodamine 123 (5 μg/mL) at 37 °C for 15 min without light, and washed twice with phosphate butter solution (PBS). The cells were then incubated again in PBS at 37 °C for 30 min without light and fluorescence was then measured using flow cytometry as in Section 4.6.3. Five thousand events were evaluated per experiment and cell debris was omitted from the analysis.

4.6.6. Morphological analysis with hematoxylin–eosin staining

To evaluate nuclear morphology, treated cells were harvested, transferred to cytospin slides, fixed with methanol for 30 s, and stained with hematoxylin–eosin.

4.6.7. Morphological analysis using fluorescence microscopy

After incubation, cells were centrifuged and re-suspended in 25 μL PBS. 1 μL of an aqueous solution of 100 μg/mL acridine orange/ethidium bromide was added and the cells were observed under a fluorescence microscope (Olympus, Tokyo, Japan). Three hundred cells were counted per sample, and were classified as follows: viable cells, apoptotic cells and necrotic cells.

4.7. Statistical analysis

Data are presented as IC_{50} values with their 95% confidence intervals (CI 95%) obtained by nonlinear regression, or as mean ± SEM calculated using the GRAPHPAD program (Intuitive Software for Science, San Diego, CA). The differences between experimental groups were compared by one-way analysis of variance (ANOVA) followed by Student Newman Keuls test.

Acknowledgments

The authors wish to thank the following Brazilian governmental agencies for their financial support in the form of grants and fellowship awards: UnB, CAPES, FAPDF, CNPq, FUNCAP, FINEP and PRONEX.

Supplementary data

Supplementary data associated with this article can be found, in the online version, at doi:10.1016/j.bmc.2010.10.044.

References and notes

1. Hanahan, D.; Weinberg, R. A. *Cell* **2000**, *100*, 57.
2. Albernaz, L. C.; de Paula, J. E.; Romero, G. A. S.; Silva, M. R. R.; Grellier, P.; Mambu, L.; Espindola, L. S. *J. Ethnopharmacol.* **2010**, *131*, 116.
3. de Mesquita, M. L.; de Paula, J. E.; Pessoa, C.; de Moraes, M. O.; Costa-Lotufo, L. V.; Grougnet, R.; Michel, S.; Tillequin, F.; Espindola, L. S. *J. Ethnopharmacol.* **2009**, *123*, 439.
4. Melo e Silva, F. M.; de Paula, J. E.; Espindola, L. S. *Mycoses* **2009**, *52*, 511.
5. de Mesquita, M. L.; Grellier, P.; Mambu, L.; de Paula, J. E.; Espindola, L. S. *J. Ethnopharmacol.* **2007**, *110*, 165.
6. Ohnmacht, S.; West, R.; Simionescu, R.; Atkinson, J. *Magn. Reson. Chem.* **2008**, *46*, 287.
7. Sakai, M.; Okabe, M.; Tachibana, H.; Yamada, K. *J. Nutr. Biochem.* **2006**, *17*, 672.
8. Wada, S.; Satomi, Y.; Murakoshi, M.; Noguchi, N.; Yoshikawa, T.; Nishino, H. *Cancer Lett.* **2005**, *229*, 181.
9. Hiura, Y.; Tachibana, H.; Arakawa, R.; Aoyama, N.; Okabe, M.; Sakai, M.; Yamada, K. *J. Nutr. Biochem.* **2009**, *20*, 607.
10. Elangovan, S.; Hsieh, T.; Wu, J. M. *Anticancer Res.* **2008**, *28*, 2641.
11. Srivastava, J. K.; Gupta, S. *Biochem. Biophys. Res. Commun.* **2006**, *346*, 447.
12. Miyazawa, T.; Shibata, A.; Sookwong, P.; Kawakami, Y.; Eitsuka, T.; Asai, A.; Oikawa, S.; Nakagawa, K. *J. Nutr. Biochem* **2009**, *20*, 79.
13. Agarwal, M. K.; Agarwal, M. L.; Athar, M.; Gupta, S. *Cell Cycle* **2004**, *3*, 205.
14. Shun, M. C.; Yu, W.; Gapor, A.; Parsons, R.; Atkinson, J.; Sanders, B. G. *Nutr. Cancer* **2004**, *48*, 95.
15. Ahn, K. S.; Sethi, G.; Krishnan, K.; Aggarwal, B. B. *J. Biol. Chem.* **2007**, *282*, 809.
16. Mosmann, T. *J. Immunol. Methods* **1983**, *65*, 55.
17. Nicoletti, I.; Magliorati, G.; Pagliacci, M. C.; Grignani, F.; Riccardi, C. *J. Immunol. Methods* **1991**, *139*, 217.